Applied Catalysis B: Environmental 180 (2016) 544–550

Contents lists available at ScienceDirect

Applied Catalysis B: Environmental

journal homepage: www.elsevier.com/locate/apcatb

Effective monitoring of the electro-Fenton degradation of phenolic derivatives by differential pulse voltammetry on multi-walled-carbon nanotubes modified screen-printed carbon electrodes

Loubna Bounab[a,b,c], Olalla Iglesias[b], Marta Pazos[b], María Ángeles Sanromán[b], Elisa González-Romero[c,*]

[a] Département de Chimie, Faculté des Sciences,- Université Abdelmalek Essaâdi, 93030 Tétouan, Morocco
[b] Departamento de Ingeniería Química, Universidad de Vigo-Campus Vigo, 36310 Vigo, Spain
[c] Departamento de Química Analítica y Alimentaria, Universidad de Vigo-Campus Vigo, 36310 Vigo, Spain

ARTICLE INFO

Article history:
Received 27 February 2015
Received in revised form 2 July 2015
Accepted 7 July 2015
Available online 15 July 2015

Keywords:
m-Cresol
Dihydroxyphenols
Carbon nanotubes catalytic surface
Voltammetric analysis
Electro-Fenton degradation

ABSTRACT

This work illustrates a fast, sensitive and selective electroanalytical methodology for simultaneous determination of phenolic derivatives. Optimization of differential pulse voltammetry (DPV) conditions and electrochemical study by cyclic voltammetry (CV) of phenolics are included. Differential pulse voltammetry at screen-printed carbon electrodes (SPCE) was selected for the sensitive detection of *m*-Cresol and Tert-butylhydroquinone. The introduction of Multi-walled Carbon-Nanotubes with acid groups, MWCNT-COOH, as modifier on working SPCE enhances the performance of electrode surface with a highly catalytic activity on it, allowing a 5-fold higher sensitive analysis than unmodified SPCE, with a limit of detection as low as about 1 μM. This simple and low-cost methodology has been applied, for first time, to monitoring the electro-Fenton degradation of *m*-Cresol, giving selective information of the reactant loss and products formation. Aromatic intermediates (monohydroxy, polyhydroxy and quinone phenolic derivatives) have been identified and followed during the electrolysis process. The electro-Fenton with iron on activate carbon is 4-fold faster than with other catalyst. The results are validated by chromatographic (HPLC) technique. The electroanalytical methodology described, in conjunction with the use of small SPCE as sensor transducer, can be implemented for continuous monitoring of end-point of the electro-Fenton reaction at industrial level in wastewater remediation plants, indicating the two main stages of electro-Fenton during the electrolysis.

1. Introduction

The rapid in situ determination of phenolic pollutants and their derivatives is an important environmental challenge because of the easy penetration of such species through membranes or skins of plants, animals and humans, with toxic effects [1,2], but not all phenolics are toxics and some of them are used as additives. Fig. 1 illustrates the structure of three phenolics with different uses and properties. On one hand, thymol is one of the most important phenolic oils of thymus, an aromatic and medicinal plant with applications in pharmaceutical and food industries, which has been reported to have antibacterial, antioxidative, and mammalian age delaying properties [3]. On the other hand, tert-butylhydroquinone (TBHQ), is a highly effective synthetic antioxidant and, in food industry, it is used as preservative (E319) and the maximum TBHQ allowed is 0.02% of the weight of the food product, regulated by U.S. Food and Drug Administration [4] and by European Food Safety Authority [5]. In opposite way, cresols are classified by the US Environmental Protection Agency (US-EPA) as pesticide, showing chronic effects at 12 mg L^{-1} of the quantitative structure–activity relationship [6], being the most toxic the *p*-Cresol isomer while the *m*-Cresol is the less of the three isomers.

The US-EPA [7] and the European Environmental Agency (EEA) [8] include eleven substituted phenols classified as hazardous for human health and assigns them a maximum admissible concentration range of 60–400 μg/L in relation with their toxicity degree. Thus, such situation requires the development of economic and ecological techniques to eliminate phenolics in contaminated environment.

* Corresponding author. Fax: +34 986 812 322.
E-mail addresses: bounabensa@gmail.com (L. Bounab), olaiaic@uvigo.es (O. Iglesias), mcurras@uvigo.es (M. Pazos), sanroman@uvigo.es (M.Á. Sanromán), eromero@uvigo.es (E. González-Romero).

http://dx.doi.org/10.1016/j.apcatb.2015.07.011
0926-3373/

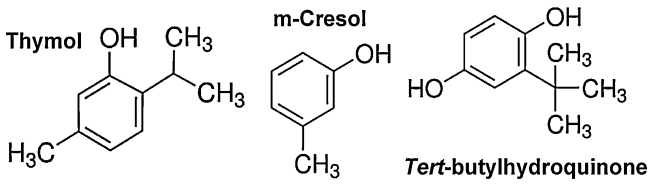

Fig. 1. Structures of phenolics used in this work (source: Sigma–Aldrich Chemicals).

In this context, removal of phenolic derivates from industrial wastewater has generated considerable attention of societiy and achieving a safety level (0.1–1.0 mg L^{-1}) is difficult 9. Recently, advanced oxidation processes (AOPs), which can produce oxidizing hydroxyl radicals, have proved to be an efficient procedure for the treatment of different organic pollutants such as phenolic derivates [10,11]. Among them, electro-Fenton have received great attention for the removal of harmful organics in waters due to the advantages of this treatment such as continuous electrogeneration of H_2O_2, a short reaction time and Fe^{2+} generation by direct reduction of Fe^{3+} on the cathode [12,13]. One of the advantages of the foam materials is their high reaction surface. Based on previous paper [14], using nickel foam as cathode, the production of hydroxyl radicals is improved. Furthermore, there is not leaching of nickel ions because the regeneration of Ni^{2+} on Ni over the influence of an electric field is possible. For this reason, the electrode keeps its structure and composition along the treatment. In order to improve the efficiency of this treatment the use of heterogeneous electro-Fenton process has been postulated. Nowadays, different catalysts have been used in heterogeneous electro-Fenton reactions such as iron–alginate gel, iron–carbon, iron–zeolite, magnetite, iron–hydrogels. [15–19]. By use of heterogeneous catalysis the reuse of iron and the operation in continuous mode are possible [15,20].

A number of methods have been developed to monitor electro-Fenton degradation, where GC–MS [21,22], UV–vis spectroscopy [19], HPLC and IC [23,24] are the most common techniques to follow the evolution of electrolysis; however, little attention has been paid to the use of electroanalytical techniques [25,26] and to our knowledge no references were found to monitor degradation of cresols.

The electronalytical techniques, in particular Cyclic (CV) and Differential Pulse Voltammetry (DPV), are good tools for the study of electrochemical mechanisms and for the sensitive detection and quantification of pollutants [27], respectively, being possible to reach detection limits as low as ppt level [28] and to apply directly to opaque media giving information of reactant and products. The selectivity shown by the DPV technique is the other advantage. Furthermore, voltammograms can reflect all oxidation/reduction steps of electroactive compounds and valuable information not only on the parent substrate but also on the electrochemically-generated species that can concurrently be obtained [29–31].

In this work, the electrocatalytic behavior of MWCNT-SPCE towards the oxidation of phenolic derivatives (TBHQ, thymol and *m*-Cresol) is described. In addition, the electrochemical mechanism in the electrooxidation of phenolics for their detection is investigated using CV and DPV. The applications of the modified SPCE with MWCNT as the catalytic sensor in the voltammetric detection of *m*-Cresol, and for the selective detection of *m*-Cresol in presence of TBHQ additive were also investigated. Finally, this optimized methodology was applied to monitor the electro-Fenton degradation of *m*-Cresol. Thus, the rate constant determination can be obtained electrochemically by monitoring directly *m*-Cresol loss and, simultaneously, by monitoring the product generation. Then, the electrochemical measurements have been proved to be a powerful tool to study the mechanism of this type of reaction since they allow the determination of rate constants and, depending on the nature of the phenolic derivative, the estimation of product yields, as has been carried out in this study. Furthermore, reliable information about the incorporation of this methodology to monitor the electro-Fenton has been collected. The use of screening technique for fast identification of the two main stages during electrolysis: aromatic intermediate and carboxylic acids production, which could be useful for researchers working in this field, is extensively discussed.

2. Material and methods

2.1. Reactants

Reagents were of maximum purity available and were used without further purification. *m*-Cresol, thymol and tert-butylhydroquinone (TBHQ) were purchased from Aldrich. The chemicals used in the preparation of the universal phosphate buffer solution, PBS, were purchased from Fluka. All solutions were prepared by using Milli-Q grade water. The phenolic stock solutions (stored in amber Eppendorf tubes at −20 °C) were diluted to the required concentration by the electrolyte (0.1 M of PBS at pH 2 or electro-Fenton electrolyte, typically 0.01 M Na_2SO_4/H_2SO_4 at pH 2). All reagents used in the electro-Fenton assays were provided by Sigma–Aldrich.

2.2. Voltammetric analysis

Cyclic and Differential Pulse Voltammetric measurements were obtained with a potentiostat/galvanostat AUTOLAB PGSTAT10 connected to the SPCE, through a connector DropSens DSC, where the electrochemical cell is placed, in conjunction with the three electrode systems described below. The system was controlled by General Purpose Electrochemical experiments software 4.9 (GPES 4.9). The cell configuration consists of working electrode: carbon (DRP-C110) and MWCNT-COOH as modifier on carbon (DRP-C110CNT) from DropSens Company (Spain), with a 4 mm diameter; a pseudo-reference electrode of silver, and a carbon counter electrode. The volume dispense on is 50 μL, enough amount to cover the three electrodes system. All potentials given hereafter will be relative to above mentioned Ag pseudo-reference electrode. The voltammetric measurements were carried out under room temperature.

The CVs were usually recorded in the potential range from −0.5 to +1.3 V, that is, $\Delta U = 1.8$ V, with a scan rate of 50 mV s^{-1} and a step potential of 5 mV, unless otherwise indicated. When using DPV, the conditions were as follows: step potential of 5 mV; pulse amplitude, ΔE, of 50 mV, modulation time of 0.05 s, interval time of 0.5 s; and scan rate of 9.9 mV s^{-1}. The potential was scanned, usually from −0.3 to +1.5 V. The residual current measurements were carried out in a quiescent solution of electrolyte in presence of oxygen. A "cleaning" step was required between successive runs and previously to any measurement. For that, 5 cycles by CV in the potential range from −1.0 to +1.5 V at 50 mV s^{-1} in 0.1 M H_2SO_4 solution was applied.

2.3. Electro Fenton remediation

The heterogeneous electro-Fenton degradation of *m*-Cresol was carried out in a cylindrical glass reactor with a working volume of 0.15 L at room temperature. The electric field was applied by a 1.6 mm thick nickel foam cathode (Goodfellow Cambridge Ltd, United Kingdom) and a BDD anode (DIACHEM®, Germany). The electrodes (surface 11 cm^2) were placed opposite to each other at 1 cm above the bottom of the cell and with an electrode gap of

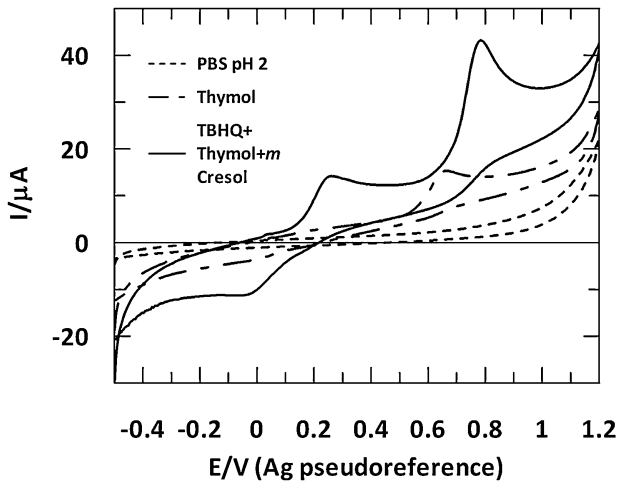

Fig. 2. Representative CV voltammograms on SPCE of solutions with 1 mM of thymol (dashed–dotted line) and ternary mixture of 1 mM of each thymol, *m*-Cresol and TBHQ (line) in 0.1 M of PBS at pH 2. Residual current (dashed line).

6 cm. A constant potential drop was applied with a power supply (HP model 3662). Current intensity was monitored along the process with a multimeter (Fluke 175). Continuous saturation of air at atmospheric pressure was ensured by bubbling 1 L/min of compressed air near the cathode.

Reaction mixture of electro-Fenton treatment contains 3 g of active carbon loaded with iron (27.6 mg/L) (Fe–AC), used as catalyst, electrolyte Na_2SO_4 (0.01 M) and *m*-Cresol (100 mg/L). In these experiments the pH was 2, modified by adding H_2SO_4. The reaction mixture as well the catalyst were placed into de cylindrical glass reactor, where the two electrodes, Ni-foam cathode and BDD anode, were immersed as described before.

DPV voltammetric kinetic data for *m*-Cresol and for the products generated in the degradation process by electro-Fenton were obtained by using the methodology described in Section 2.2. Aliquots of 50 μL of the electro-Fenton reaction mixture were transferred to the screen-printed electrode at convenient intervals of time. After each aliquot was dispensed on the unmodified or MWCNT modified SPCE, the DPV voltammogram was recorder at the optimized conditions, scanning a window potential from −0.3 to +1.5 V.

3. Results and discussion

3.1. Characterization of working electrode surface by scanning electron microscopy (SEM)

Voltammetric behavior of monohydroxy- and polyhydroxy-phenolic derivatives was investigated using CV and DPV on SPCE and on modified MWCNT-SPCE with –COOH terminal groups attached to the MWCNT. The characterization of both electrode surfaces was carried out by scanning electron microscopy (SEM) (see method and Fig. S1 in Supplementary data). The commercial SPCE (Fig. S1A) presents a heterogeneous nanometric granular surface characteristic of carbon black, but the surface of the MWCNT-SPCE micrograph (Fig. S1B) shows a randomly distributed multilayer of MWCNTs on the surface as consequence of no control over the assembly of CNTs during the drop-casting process and it looks like a porous carbon electrode [32].

3.2. CV Studies of phenolic derivatives

In the studies by CV on SPCE as working electrode in 0.1 M PBS (pH 2), the thymol (Fig. 2) exhibits one and well defined

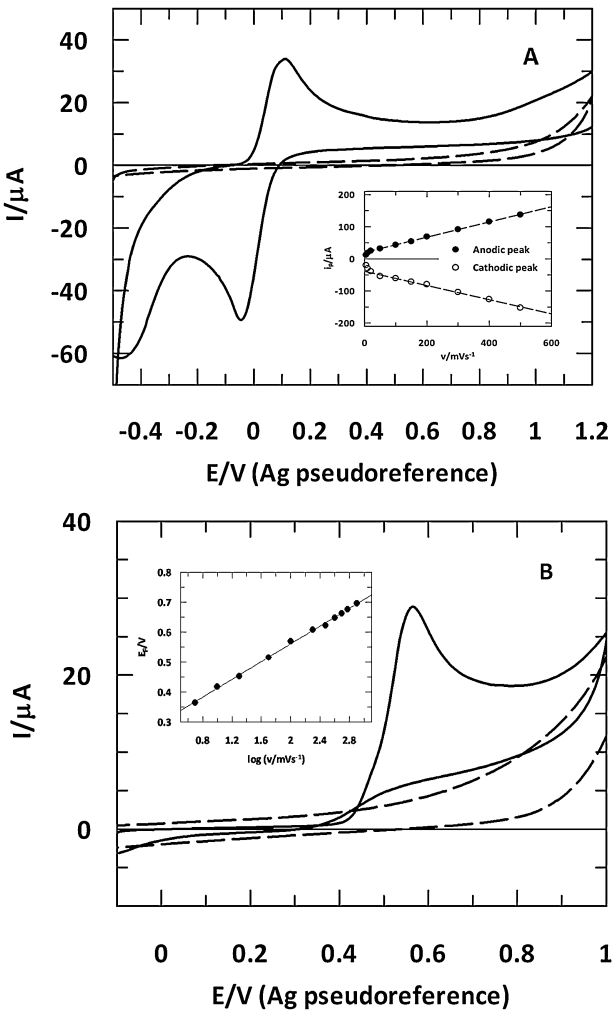

Fig. 3. Representative CV voltammograms on MWCNT-SPCE of solutions with 1 mM of both TBHQ (A) and *m*-Cresol (B) in 0.1 M of PBS at pH 2. Residual current (dashed line). Inset A: dependence of peak current with scan rate for TBHQ. Inset B: dependence of peak potential with logarithm of scan rate for *m*-Cresol.

one-electron irreversible oxidation peak at about 0.657 V with i_{pa} of 8.2 μA, when the potential was scanned between −0.5 V and 1.2 V (Fig. 2). The same Fig. displays the CVs of the ternary mixture of TBHQ, thymol and *m*-Cresol at the SPCE. It can be seen that the voltammetric peaks of thymol and *m*-Cresol (monohydroxy derivatives) overlapping severely on SPCE and showed only one peak at 0.784 V. However, it is easy to locate the oxidation peak of TBHQ (dihydroxy derivative) at lower potentials, *c.a.* 0.257 V, and also a reduction peak at −0.026 V at reverse scan appeared for this polyphenol, characteristic for dihydroxyl containing aromatic compound as hydroquinone or dopamine, that is oxidized by a quasireversible two electron redox mechanism [33,34].

The electrochemical reactions of TBHQ, thymol and *m*-Cresol on SPCE modified with MWCNT-COOH were also investigated (Fig. 3). The voltammograms for TBHQ and *m*-Cresol display a marked improvement when the MWCNT-SPCE is used. The oxidation potential is located at 0.110 V for TBHQ (Fig. 3A); it also shows the reduction potential at −0.046 V, with a peak-to-peak separation (ΔE_p) of 156 mV and with the anodic and cathodic peak currents of 31 μA and 48 μA, respectively, and another wave at about −0.5 V is shown in the voltammogram of TBHQ. The latter can be attributed to both the reduction of the electrogenerated product in the first reduction process at −0.046 V or the fast coupling chemical reaction. For *m*-Cresol (Fig. 3B), the oxidation potential

is located at 0.564 V with the anodic peak current of 27 μA and no reduction peak is observed in the reverse scan. In conclusion, the MWCNT-SPCE has notable improvements in their electrochemical performance, with respect to unmodified SPCE. The peak currents for both phenolic derivatives increased up to 5 times, which is representing an increase of sensor sensibility. Furthermore, the relevant peak potential shifts to cathodic direction occurred for the oxidation peaks of TBHQ (*c.a.* 147 mV) and *m*-Cresol (*c.a.* 220 mV), together with the change of peak shape (sharper and more symmetric), demonstrate the modification in nature of electrochemical process and more favored electron transfer kinetics take place on MWCNT-SPCE. The improvements can be explained by the well-known catalytic properties of MWCNT and the effect of terminal –COOH groups anchored to the MWCNT on hydroxyl groups from the phenolic [32,35]. The binary mixture of thymol and *m*-Cresol gives only one broad oxidation peak about 0.6 V (results not shown) in the same way that obtained on SPCE. Therefore, it is not possible to detect both components individually, but it is easy to determine selectively the monohydroxyl and dihydroxyl phenolic derivatives in the mixture.

More detailed experimental studies were carried out about characteristic of oxidation of these phenolics on MWCNT-SPCE to get insight about their electrochemical process and on the electron transfer kinetics. First of all, influences of potential scan rate on peak potential and peak current were studied for TBHQ (Fig. 3, inset A and Fig. S2 in Supplementary data) and *m*-Cresol (Fig. 3, inset B and Fig. S3 in Supplementary data). As could be seen in Fig. 3, inset A for TBHQ, a linear relationship was obtained between the anodic and cathodic peaks and the scan rate in the range of 5–500 mV s^{-1}; this revealed that both oxidation and reduction were rather an adsorption-controlled step than a diffusion-controlled process [28,36]. The voltammograms at different scan rates are shown in Fig. S2 in Supplementary data. It can be seen that one oxidation peak and two reduction peaks are observed at slow scan rates, which become to one oxidation and one reduction peaks at faster scan rates. The reason is as follows: the TBHQ is easily oxidized to TBQ that is transformed into non oxidizable specie (second reduction peak), which revealed that a strong adsorption of the product is involved in the overall electrochemical process. As the voltammogram is recorder faster, the TBQ does not have time to adsorb and therefore the second reduction peak is not detected [37]. The graph of the peak potential vs the logarithm of scan rate show a formal potential, $E^{0\prime}$, of (19 ± 3) mV and that the peak separation increases as the scan rate becomes faster, yielding straight lines, indicating a charge transfer kinetics limitation. The charge-transfer coefficient (α_a) and the electron transfer kinetic constants (k_{ET}) of TBHQ were determinate from the plots, in accordance with Lavironís theory [38]. Thus, values of 0.20 and 1.77 s^{-1} were estimated for α_a and k_{ET}, respectively, which are in good agreement with the values calculated by Gusmão et al. for other dihydroxyl phenolic derivatives [33]. Table S1 (Supplementary data) shows the equations of peaks currents and peak potentials for TBHQ and the scan rate study.

As could be seen in Fig. 3, inset B for *m*-Cresol, peak potential shifts to more anodic values with increasing scan rate confirming the irreversibility of oxidation under investigation and supporting a kinetic limitation for the reaction between the redox sites of –COOH from the modifier MWCNTs and the *m*-Cresol. For this kind of mechanism, a linear relationship between the peak potential (E_p) and logarithm of scan rate can be found and from the slope of E_p vs log v, expressed as Eq. (1) [3,39] and as shows inset B of Fig. 3.

$$E_P = \left(\frac{b}{\alpha n}\right) * \log v + cte \quad (1)$$

The linear fitting between the peak potential and logarithm of scan rate follows the equation: E_{pa} (V) = (0.264 ± 0.005) + (0.148 ± 0.002) log v (mVs^{-1}) (square regression coefficient R^2 = 0.9991). The evaluated slope of Ep vs log v is then 148 mV, and according to the theory of [38], the value of $\alpha_a n$ was calculated as 0.40, where n = 0.80 (≅1e^-) indicating that the one electron transfer is the rate-limiting step (assuming a transfer coefficient of α_a = 0.5 for totally irreversible process) [3,40]. Effects of scan rate on peak current were also investigated. As scan rate increase from 0.005 to 0.5 Vs^{-1} at fixed concentration of *m*-Cresol (Fig. S3 in Supplementary data), the peak current is not proportional to the square root of scan rate (Fig. S3, inset A) that is expected for reactions that involve mass transport and it is totally diffusion controlled, but the peak current is found to be changed linearly with the scan rate (Fig. S3, inset B), with a linear relationship: i_{pa} (μA) = (14.4 ± 0.7) + (0.098 ± 0.003) v ($mV\,s^{-1}$) (R^2 = 0.997), indicating the effect of adsorption mechanism [28,36].

On the other hand, the influence of number of scans is also studied and the results are shown in Fig. S4 and S5 (Supplementary data) for TBHQ and *m*-Cresol, respectively. The study illustrates the behavior of polyhydroxyl and monohydroxyl phenolic derivatives as a representative example. As shown in Fig. S4 for TBHQ, with the increase in the cycle number of voltammetric scans, one oxidation peak was observed at about 0.1 V and two reductions peaks were gradually observed at about 0.0 V and −0.3 V, respectively. The peak current increased with the enhancement of the cyclic number of voltammetric scans, indicating that an electroconductive film was formed on the electrode surface by potential cycling between −0.5 and +1.3 V [28,41,42]. In contrast, the anodic peak for *m*-Cresol (Fig. S5 in Supplementary data) shows an initial peak current in the first voltammetric scan that decrease about a 74% in the second voltammetric scan. The peak current of *m*-Cresol decreases with continued potential cycling and this peak fully disappears at the voltammetric scan number 10. This behavior is consistent with the formation of an insoluble polymer film resulting in passivation of the electrode [43–45]. If the solution is removed from the MWCNT-SPCE surface, rinsed with water, and a fresh 50 μL of 0.1 M PBS at pH 2 is placed on the electrode surface, a voltammetric peak of *m*-Cresol is observed, with a peak current equivalent to the high of peak at scan number 5 in Fig. S5 (red line) in Supplementary data. These behaviors suggest a strong interactions of phenolic derivatives with the active functional groups on working electrode surface, in good agreement with the results obtained with the scan rate study, being necessary a "cleaning step" to remove the *m*-Cresol adsorbed or the film formed with TBHQ on electrode surface just before a new use of the electrode, at the same time, an activation of the modified electrode surface was achieved with this treatment, generating a catalytic surface with an increasing of active area, doing the detection more sensitive.

3.3. DPV Studies on MWCNT-SPCE

To obtain a much more sensitive peak current, DPV on MWCNT-SPCE was applied (Fig. 4). Fig. 4A illustrates the DPV voltammograms for thymol, *m*-Cresol and ternary mixture of the three phenolic derivatives at the optimized instrumental conditions.

It can be see that the voltammetric peaks of thymol and *m*-Cresol overlapping severely on MWCNT-SPCE and showed only one peak at about 0.520 V. However, it is easy to locate the oxidation peak of TBHQ at lower potentials, *c.a.* 0.0 V, such as was also indicated in CV studies, but with higher peak separation (*c.a.* about 520 mV by DPV vs 450 mV by CV) between the dihydroxy and monohydroxy derivatives, doing more selective the analysis.

In order to obtain the concentration range in which the response of the electrode is linear with the concentration and the detection and quantification limits, the effect of concentration of *m*-Cresol

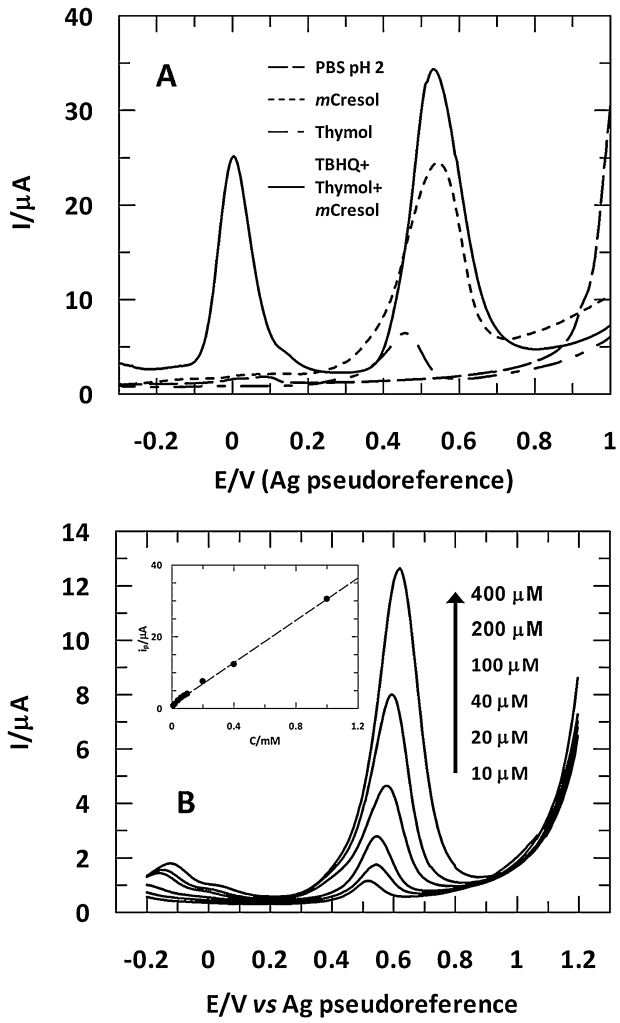

Fig. 4. DPV voltammograms obtained with 0.5 mM of thymol (dashed–dotted line), 1 mM of *m*-Cresol (dotted line) and ternary mixture of 0.5 mM thymol, 1 mM *m*-Cresol and 1 mM TBHQ (line) (A) and DPV voltammograms obtained with *m*-Cresol at different concentration (B) in 0.1 M of PBS at pH 2 on MWCNT-SPCE. Inset B: Calibration graph for the *m*-Cresol.

on peak currents was investigated. Fig. 4B shows the differential pulse voltammograms relative to the *m*-Cresol at different concentrations and inset the corresponding calibration graph. The calibration curve exhibits a linear relation between the peak current of *m*-Cresol at about 550 mV and its concentration over the range 10 µM–1 mM. Statistical analysis gave the following equation: i_{pa} (µA) = (0.99 ± 0.16) + (0.0295 ± 0.0004) (*m*-Cresol) (µM) (R^2 = 0.9992). The detection and quantification limits, calculated as three and ten times the standard deviation of residual current and slope of calibration curve ratio, were found to be 1.4 µM and 4.6 µM, respectively.

3.4. DPV monitoring of electro-Fenton degradation of m-Cresol

Here the electro-Fenton degradation of *m*-Cresol in 0.01 M Na_2SO_4/H_2SO_4 at pH2 was examined by employing DPV on modified MWCNT-SPCE combined with the optimized voltammetric method. The relationship between DPV peak current and concentration was also found to be linear i_{pa} (µA) = (1.29 ± 0.0.45) + (0.038 ± 0.002) (*m*-Cresol) (µM) (R^2 = 0.997) at 563 mV over the range 0.01–0.90 mM (100 mgL^{-1}) under electro-Fenton conditions. Limits of detection and quantification were found to be 2.7 µM and 9.1 µM, respectively.

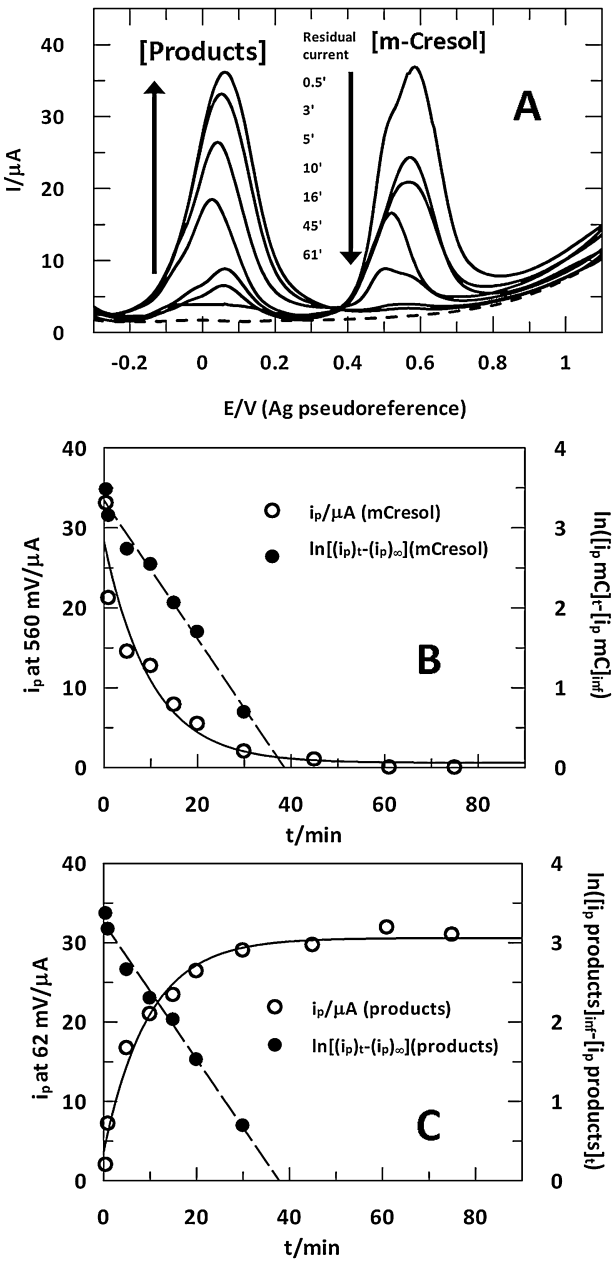

Fig. 5. Monitorization of electro-Fenton degradation of *m*-Cresol by DPV on MWCNT-SPCE (A) and determination of the observed rate constants by monitoring the decrease in the peak current for the voltammetric peak at 560 mV for *m*-Cresol (B) and the increase in the peak current for the voltammetric peak at 62 mV for the generation of products (C) with the corresponding linear plots according to equation S1 in Supplementary material (black symbols in both graphs). Initial concentration of *m*-Cresol 100 mg/L in presence of 27.6 mg/L of iron in [H_2SO_4/Na_2SO_4] = 0.01 M at pH2.

Fig. 5 illustrates the evolution of the voltammograms and the peak currents values during the electro-Fenton degradation of 100 mg/L (0.92 mM) of *m*-Cresol. During the first positive scan at 0.5 min (Fig. 5A), an anodic peak was observed at about 0.560 V and this peak was attributed to the oxidation of *m*-Cresol. For this first scan, a shoulder at lower potentials can be also observed. Upon further scans at different electrolysis times, the anodic peak shifted to a more negative potential while the shoulder was unaltered and eventually coalesced into a broad anodic peak centered at about 0.50 V and its anodic peak currents decreased, indicating continuous degradation of monohydroxyl derivative. The last scan recorded at 61 min of electrolysis time shows no peak around

0.5 V. (also illustrated in Fig. 5B). At the moment, there is no clear explanation for the emergence of this shoulder, but it could be associated with the aromatic radical intermediate generated during the electrolysis. It can be also seen in the same figure that, during the successive scans from 0.5 min up to 10 min of electrolysis times, a second anodic peak appeared at a potential around 0.0 V with a shoulder at lower potential (*c.a.* −0.02 V) that were attributed to the oxidation of the generated products in the electro-Fenton reaction. After 10 min of electro-Fenton reaction, the voltammograms show a unique peak for product generation. This broad peak increased gradually on subsequent scans and then became constant up to 30 min (illustrated also in Fig. 5C). It is known that the peak potential sequence for oxidation of dihydroxyl benzene derivatives is hydroquinone, catechol and resorcinol and that the easier oxidation for hydroxyl substituent is in the *para*-position [46]. TBHQ has a peak potential at about 0.0 V at pH2 (this paper) and the peak potential for dopamine (catecholamine derivative) happens at higher potential values than catechol by itself [33]. Therefore, it may be predicted that, during *m*-Cresol electrolysis, the main initial reactions would successively electrophilic additions of hydroxyl radical on the aromatic ring, leading to competitive paths with the most probable radical attack to the *ortho* and *para* positions (preferred). Thus, this leads to the generation of 3-methylcatechol and 2-methylhydroquinone as main species, which generates the degradation of cresols under our experimental conditions at the beginning of electro-Fenton. At the end of the first stage of the electrolysis, the main produced product is 2-methylhydroquinone. This fact is in good agreement with the studies presented by other authors expert in the field [6,21,47].

As shown before, at a specific pH and electrolyte, the diffusion currents are proportional to (*m*-Cresol). Therefore, a MWCNT-SPCE electrode can be used as sensor to determine phenolics both qualitatively (by the peak potential value) and quantitatively (by comparing the measured diffusion current with the calibration plot obtained from diffusion current-phenolic concentration profile). In Fig. 5 is also illustrated the determination of the observed rate constants, k_{obs}, for the electro-Fenton degradation of *m*-Cresol (Fig. 5B) and the generation of products (Fig. 5C). The constant was obtained by fitting to both pseudo-first order reaction and integrated first order equation S1 (see method for kinetic data analysis in Supplementary data) the variation of i_p for the oxidation peaks of *m*-Cresol at 560 mV and of the generation of products at 62 mV with time. For *m*-Cresol loss, the values are k_{obs} $(9.9 \pm 0.4) \times 10^{-2}$ min^{-1} (*pseudo-first order*) and k_{obs} $(8.7 \pm 0.6) \times 10^{-2}$ min^{-1} (*integrated*, $R^2 = 0.993$) while for products production they are k_{obs} $(10.3 \pm 1.2) \times 10^{-2}$ min^{-1} (*pseudo-first order*) and k_{obs} $(8.6 \pm 0.4) \times 10^{-2}$ min^{-1} (*integrated*, $R^2 = 0.993$). It can be observed that the values of k_{obs} from *m*-Cresol loss and product generation are equals, within experimental error, and then a very reactive radical intermediate is formed during the degradation of *m*-Cresol to generate 2-methylhydroquinone as main product [6,21], being the products yield up to 92% after half an hour of electrolysis, and the degradation rate of m-Cresol under our electro-Fenton conditions, using as catalyst iron on activated carbon (Fe-AC), was faster around 4-fold than reported in the literature [21].

To validate our results, the values of k_{obs} were compared with those obtained by employing other analytical techniques, and we found that they are in perfect agreement with those obtained by HPLC ($(9.4 \pm 0.4) \times 10^{-2}$ min^{-1}) under same electro-Fenton conditions [48].

Once the *m*-Cresol is converted to 2-methylquinone during the first stage of the oxidation process by electro-Fenton, the next function of hydroxyl radicals in situ generated is to break the aromatic ring to generate carboxylic acids in a second stage of electrolysis. Fig. 6 illustrates the voltammograms at the beginning for this second stage at a wide window potential, that is, at the earlier time of the second stage during the electrolysis after *m*-Cresol is lost. The peak at about 1.35 V (closer to solvent evolution) starts to appear once the peak of *m*-Cresol disappears and it can be attributed to the carboxylic product. This is due to collateral reactions of the radicals generated during the electrolysis with the main reaction product (2-methylhydroquinone/2-methylquinone reversible system) to produce the break of aromatic ring and the generation of these carboxylic acids, whose oxidation is more difficult. On the other hand, it can follow the reduction reactions (scanning the potential range from 0.5 to −1.5 V on SPCE) of 2–methyl-p-benzoquinone to 2-methylhydroquinone and both *trans*- and *cis*- isomers, fumaric and maleic acids, to succinic acid [49]. Others carboxylic acids as formic and oxalic acids (end products before total mineralization) can be affect to the anodic oxygen evolution window. However, this is not conclusive and additional longer electrolysis time should be monitored (experiments in course).

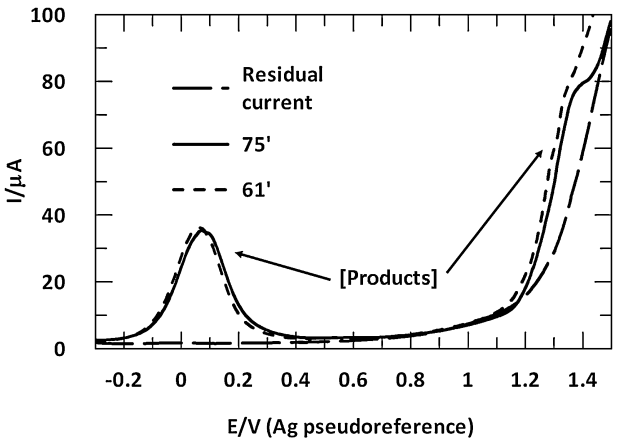

Fig. 6. DPV voltammograms with time at the end of the monitored electro-Fenton degradation of *m*-Cresol. $[H_2SO_4/Na_2SO_4] = 0.01$ M at pH2.

4. Conclusions

The speed of the analysis of a reaction mixture and the possibility to carry out real time analysis directly in the reaction mixture makes DPV very useful in kinetic studies of degradation of phenolics, complementing other techniques like UV–vis spectroscopy and chromatography (HPLC). Limits of detection as low as about 1 μM, as those found in this work, are low enough for kinetic studies, nevertheless lower limits can be achieved by modifying instrumental conditions upon more demanding applications. The composite results together with the variety of different voltammetric peaks available to monitor this kind of reactions suggest that both DPV and CV at the SPCE are one of the simplest, feasible, and relatively cheap techniques available to detect and to quantify selectively phenolic derivatives in opaque solutions and to investigate their reaction mechanisms, especially those involving electron transfer. Then, this methodology can be used *in tandem* with others to get insight the evolution of the electro-Fenton degradation process of phenolic and, simultaneously, have knowledge of the mechanism involved on it. The application of the electroanalytical technique, in conjunction with the use of small SPCE as sensor transducer, can be used for continuous monitoring of end-point of the electro-Fenton reaction at industrial level in wastewater remediation plants and it can indicate the two main stages of electro-Fenton during the electrolysis. Finally, the use of very small sample volumes (50 μL) to monitor the remediation process, together with no generating great amounts of solvent residues, makes this methodology very attractive and environmentally friendly.

Summarizing the above results, we confirm that the MWCNT modified screen-printed electrodes act catalytically in phenolics detection by DPV and Fe–AC acts as an excellent catalyst in the heterogeneous electro-Fenton degradation of these compounds; complete removal was observed at 30 min.

Acknowledgement

Financial support from the following Spanish institutions is acknowledged: MINECO (CTQ2011-28157 and CTM2011-26423/ERDF Funds), Xunta de Galicia (XUGA/FEDER R2014/030) and Universidad de Vigo. LB acknowledges to Erasmus Mundus Green IT Program from EACEA-European Union (REF: 2012-2625/001-001-EM-Action2-Partnerships-Staff mobility 2014).

Appendix A. Supplementary data

Supplementary data associated with this article can be found, in the online version, at http://dx.doi.org/10.1016/j.apcatb.2015.07.011

References

[1] M.L. Davì, F. Gnudi, Water Res 33 (1999) 3213–3219, http://dx.doi.org/10.1016/S0043-1354(99) 27-5
[2] M. Li, Y.T. Li, D.W. Li, Y.T. Long, Anal. Chim. Acta. 734 (2012) 31–44, http://dx.doi.org/10.1016/j.aca.2012.05.018
[3] X. Zhao, Y. Du, W. Ye, D. Lu, X. Xia, C. Wang, New J. Chem. 37 (2013) 4045–4051, http://dx.doi.org/10.1039/c3nj01059g
[4] Administration, U. S. F. a. D., in: U.S. Food and Drug Administration (Ed.), Food and Drugs Chapter I-Food and Drug Administration Department of Health and Human Services, U.S. Food and Drug Administration, 2014.
[5] E.F.S. Authority 84 (2004) 1–50.
[6] C. Flox, C. Arias, E. Brillas, A. Savall, K. Groenen-Serrano, Chemosphere 74 (2009) 1340–1347, http://dx.doi.org/10.1016/j.chemosphere.2008.11.050
[7] E.P. Agency October 26, Part VIII, 40 cfr (1984) 58.
[8] E.E. Agency, EEA Tech.Rep. 8 (2011).
[9] T. Soltani, M.H. Entezari, Chem. Eng. J. 251 (2014) 207–216, http://dx.doi.org/10.1016/j.cej.2014.04.021
[10] C. Flox, E. Brillas, A. Savall, K. Groenen-Serrano, Curr. Org. Chem. 16 (2012) 1960–1966, http://dx.doi.org/10.2174/138527212803251712
[11] E. Brillas, C.A. Martínez-Huitle, Appl. Catal. B 166–167 (2015) 603–643, http://dx.doi.org/10.1016/j.apcatb.2014.11.016
[12] I. Sirés, E. Brillas, M.A. Oturan, M.A. Rodrigo, M. Panizza, Environ. Sci. Pollut. Res. 21 (2014) 8336–8367, http://dx.doi.org/10.1007/s11356-014-2783-1
[13] Y. Wang, Y. Liu, K. Wang, S. Song, P. Tsiakaras, H. Liu, Appl. Catal. B 165 (2015) 360–368 http://dx.doi.org/10.1016/j.apcatb.2014.09.074
[14] W. Liu, Z. Ai, L. Zhang, J. Hazard. Mater. 243 (2012) 257–264, http://dx.doi.org/10.1016/j.jhazmat.2012.10.024
[15] O. Iglesias, M.A. Fernández de Dios, M. Pazos, M.A. Sanromán, Environ. Sci. Pollut. Res. 20 (2013) 5983–5993, http://dx.doi.org/10.1007/s11356-013-1610-4
[16] C. Zhang, M. Zhou, G. Ren, X. Yu, L. Ma, J. Yang, F. Yu, Water Res. 70 (2015) 414–424, http://dx.doi.org/10.1016/j.watres.2014.12.022
[17] M.Á. Fernández De Dios, O. Iglesias, M. Pazos, M. Á. Sanromán, Sci. World J. 2014 (2014), http://dx.doi.org/10.1155/2014/801870
[18] P.V. Nidheesh, R. Gandhimathi, S. Velmathi, N.S. Sanjini, RSC Adv. 4 (2014) 5698–5708, http://dx.doi.org/10.1039/c3ra46969g
[19] E. Bocos, M. Pazos, M.A. Sanromán, J. Chem. Technol. Biotechnol. 89 (2014) 1235–1242, http://dx.doi.org/10.1002/jctb.4374
[20] E. Rosales, O. Iglesias, M. Pazos, M.A. Sanromán, J. Hazard. Mater. 213–214 (2012) 369–377, http://dx.doi.org/10.1016/j.jhazmat.2012.02.005
[21] Y. Chu, D. Zhang, L. Liu, Y. Qian, L. Li, J. Hazard. Mater. 252–253 (2013) 306–312, http://dx.doi.org/10.1016/j.jhazmat.2013.03.018
[22] C. Flox, P. Cabot, F. Centellas, J.A. Garrido, R.M. Rodríguez, C. Arias, E. Brillas, Appl. Catal. B 75 (2007) 17–28 http://dx.doi.org/10.1016/j.apcatb.2007.03.010
[23] M.A. Oturan, N. Oturan, C. Lahitte, S. Trevin, J. Electroanal. Chem. 9 (2001) 6–102, http://dx.doi.org/10.1016/S0022-0728(01) 369-2
[24] O. Iglesias, J. Gómez, M. Pazos, M.A. Sanromán, Appl. Catal. B 144 (2013) 416–424, http://dx.doi.org/10.1016/j.apcatb.2013.07.046
[25] A.C. de Andrade Lima, E.G. da Silva, M.O.F. Goulart, J. Tonholo, T.T. da Silva, F.C. de Abreu, J. Braz. Chem. Soc. 20 (2009) 1698–1704.
[26] X. Wang, K. Jiao, Anal. Chim. Acta. 664 (2010) 34–39, http://dx.doi.org/10.1016/j.aca.2010.02.005
[27] S. Radhakrishnan, K. Krishnamoorthy, C. Sekar, J. Wilson, S.J. Kim, Appl. Catal. B 148–149 (2013) 22–28, http://dx.doi.org/10.1016/j.apcatb.2013.10.044
[28] J. Wang, Analytical Electrochemistry, VCH, Berlin, 2000.
[29] E. González-Romero, B. Malvido-Hermelo, C. Bravo-Diaz, Langmuir 18 (2002) 46–55, http://dx.doi.org/10.1021/la010938l
[30] C. Bravo-Díaz, E. González-Romero, Electroanalysis 15 (2003) 303–311, http://dx.doi.org/10.1002/elan.200390038
[31] E. González-Romero, B. Fernández-Calvar, C. Bravo-Díaz, Prog. Colloid Polym. Sci. 123 (2004) 131–135.
[32] P. Fanjul-Bolado, P. Queipo, P.J. Lamas-Ardisana, A. Costa-García, Talanta 74 (2007) 427–433, http://dx.doi.org/10.1016/j.talanta.2007.07.035
[33] R. Gusmão, V. López-Puente, I. Pastoriza-Santos, J. Pérez-Juste, M.F. Proença, F. Bento, D. Geraldo, M.C. Paiva, E. González-Romero, RSC Adv. 5 (2015) 5024–5031, http://dx.doi.org/10.1039/c4ra12660b
[34] Y. Zhang, J.B. Zheng, Electrochim. Acta 52 (2007) 7210–7216, http://dx.doi.org/10.1016/j.electacta.2007.05.039
[35] M. Pumera, Chem. Rec. 12 (2012) 201–213, http://dx.doi.org/10.1002/tcr.201100027
[36] C.M.A. Brett, A.M.O. Brett, Electrochemistry. Principles, Methods and Application, Oxford University Press, New York, 1993.
[37] R.H. Wopschall, I. Shain, Anal. Chem. 39 (1967) 1514–1527.
[38] E. Laviron, J. Electroanal. Chem. 101 (1979) 19–28.
[39] A. Abbaspour, M.A. Kamyabi, J. Electroanal. Chem. 576 (2005) 73–83, http://dx.doi.org/10.1016/j.jelechem.2004.10.008
[40] C.-. Xu K.-. Huang, W. W.-. Xie, Colloids Surf. B 74 (2009) 167–171, http://dx.doi.org/10.1016/j.colsurfb.2009.07.013
[41] I. Adraoui, M. El Rhaz, A. Amine, L. Idrissi, A. Curulli, G. Palleschi, Electroanalysis 17 (2005) 685–693, http://dx.doi.org/10.1002/elan.200403140
[42] K.- Huang, L. Wang, J. Li, M. Yu, Y. Liu, Microchim. Acta. 180 (2013) 751–757, http://dx.doi.org/10.1007/s00604-013-0988-5
[43] S. Myler, S. Eaton, S.P.J. Higson, Anal. Chim. Acta. 357 (1997) 55–61, http://dx.doi.org/10.1016/S0003-2670(97) 558-8
[44] M. Revenga-Parra, C. Gómez-Anquela, T. García-Mendiola, E. Gonzalez, F. Pariente, E. Lorenzo, Anal. Chim. Acta. 747 (2012) 84–91, http://dx.doi.org/10.1016/j.aca.2012.07.043
[45] M. Revenga-Parra, T. García-Mendiola, J. González-Costas, E. González-Romero, A.G. Marín, J.L. Pau, F. Pariente, E. Lorenzo, Anal. Chim. Acta. 813 (2014) 41–47, http://dx.doi.org/10.1016/j.aca.2014.01.026
[46] H. Yin, Q. Zhang, Y. Zhou, Q. Ma, T. Liu, L. Zhu, S. Ai, Electrochim. Acta 56 (2011) 2748–2753, http://dx.doi.org/10.1016/j.electacta.2010.12.060
[47] C. Flox, P.- Cabot, F. Centellas, J.A. Garrido, R.M. Rodríguez, C. Arias, E. Brillas, Appl. Catal. B 75 (2007) 17–28, http://dx.doi.org/10.1016/j.apcatb.2007.03.010
[48] L. Bounab, O. Iglesias, E. González-Romero, M. Pazos, M. Ángeles Sanromán, RSC Adv. 5 (2015) 31049–31056, http://dx.doi.org/10.1039/c5ra03050a
[49] F.M. El-Cheikh, F.A. Rashwan, H.A. Mahmoud, M. El-Rouby, J. Appl. Electrochem. 40 (2010) 79–89, http://dx.doi.org/10.1007/s10800-009-9983-2.